

The effect of different C contents on the microstructure evolution and mechanical properties of Ti45Al6Nb alloy

Hongze Fang^{1*}, Kexuan Li¹, Lingyan Zhou¹, Jiangshan Liang¹, Xiaokang Yang¹ and Ruirun Chen¹

¹School of Materials Science and Engineering, Harbin Institute of Technology, Harbin 150001, PR China

Abstract: The content of C element and in-situ Ti₂AlC phase is adjusted to reduce the content of B2 phase in the TiAl matrix, ultimately improving the compressive properties of TiAl alloys. Results show that there is a high content of B2 phase inside the lamellar colony, and the Nb content in the B2 phase is higher than that dissolved in matrix. The addition of C element results in the formation of a round rod like reinforcing phase and refining the lamellar colony. As the C content increases from 0 to 3.0 at. %, the content of in-situ Ti₂AlC reinforcing phase increases from 0 to 17.8 vol. %, the content of B2 phase decreases from 10.4 to 1.4 vol. %, and the size of the lamellar colony decreases from 161.3 to 19.5 μm. The decrease in the content of B2 phase is due to the preferential formation of Ti₂AlC reinforcing phase in the liquid, Nb will preferentially dissolve in it, resulting in a more uniform distribution of Nb in the solidified structure and reducing the segregation of Nb. Then, Ti₂AlC particles act as heterogeneous nucleation, increasing the nucleation sites in the alloy melt and refining the microstructure. According to the results of the compression test, as the C content increases from 0 to 2.5 at. %, the compressive strength increases from 1186.9 to 2154.5 MPa, and the compressive strain increases from 6.5 to 20.2 %. Therefore, the precipitation strengthening effect of Ti₂AlC, the grain boundary strengthening effect of refined microstructure, and the decrease in the content of B2 phase jointly contribute to the improvement of the compressive properties at room temperature.

1 Introduction

As a potential material for aerospace, TiAl based alloys are believed to be applicable in fields of automotive engines, gas turbines, and aerospace because of the excellent high-temperature properties such as low density, good high-temperature creep and corrosion resistance, and high specific strength [1]. Although TiAl based alloys exhibit superior high-temperature oxidation resistance and high-temperature mechanical properties compared to ordinary Ti based alloys, their resistance to high-temperature creep and high-temperature oxidation weakens when the temperature exceeds 800 °C, which restrains the further application of TiAl based alloys [2]. Adding alloying elements with high melting point to TiAl alloys is one of the methods to solve this problem, with the most typical alloy system being Ti-Al-Nb alloy [3].

The addition of Nb element effectively improves the mechanical properties at room and high-temperatures of TiAl alloy, allowing its operating temperature to be increased to 900 °C [4]. Ti-Al-Nb based alloys have excellent properties, which are closely related to their microstructure. The substitution of Ti atom by Nb atom in the matrix results in a continuously ordered structure of the alloy system. The Nb atoms dissolved in the matrix improve the microstructure and mechanical properties of the alloy. The microstructure of Ti-Al-Nb based alloys can be divided into near γ structure (NG) and full lamellar structure (FL), and the mechanical properties corresponding to the two structures are also different, mainly depending on the proportion of constituent phases [5]. Adding 10 at. % Nb to Ti₄₅Al alloy results in a near γ

* Corresponding author: fanghongze@hit.edu.cn

microstructure, and the mechanical properties at different temperatures are higher than those of ordinary Ti45Al alloy [6]. The solid solution strengthening effect of Nb element is one of the major reasons for regulating the microstructure and mechanical properties [7]. During the high-temperature deformation process of Ti-Al-Nb alloy, not only does the solid solution strengthening of Nb play an important role, but twinning becomes an effect method for the TiAl alloy to continue deformation as the strain is large and dislocation slip cannot continue [8].

In high Nb TiAl alloys, if the high-temperature β phase is retained in the final solidification structure, white B2 phase will exist at the lamellar colony boundaries or within lamellar colony [9]. This metastable B2 phase has a bcc crystallographic structure, which appears in the matrix and refines the microstructure, exhibiting great thermal workability [10]. However, the deformation coordination between B2 phase and matrix is poor as the alloy subjected to low temperatures, and then numerous microcracks will form at the phase interface, thereby reducing the mechanical properties [11]. Therefore, it is necessary to appropriately control or eliminate the B2 phase in TiAl alloys. By using composite technology to form a certain volume fraction of reinforcing phase is formed in the alloy, allowing excessive Nb elements to dissolve into the reinforcing phase, thereby controlling the content of B2 phase in the TiAl alloy matrix. This method of preparing TiAl-based composites an effective way to improve the alloy structure, and the addition of C element is a commonly used element in this method [12]. When the C content exceeds the limit solubility of the matrix, TiC or Ti_x+AlC_x precipitates will be formed during the solidification process. The Ti_x+AlC_x precipitate formed by in-situ reaction results in better interfacial bonding [13]. Therefore, the in-situ reaction to form carbides in the TiAl matrix is utilized in this study, thereby controlling, or eliminating the B2 phase, and then improving the microstructure, ultimately enhancing the mechanical properties. The effects of different C content on the microstructures, relative content of carbides, phase composition, and compressive properties at room temperature are investigated, the mechanisms by which C for the microstructure evolution and mechanical properties are revealed.

2 Materials and methods

The raw materials of the prepared TiAl alloys included sponge titanium (purity of 99.9%), high-purity aluminum (purity of 99.9%), graphite powder (purity of 99.9%), and AlNb master alloy (mass fraction of Nb is 70 wt. %). Preparation of Ti45Al6NbxC ingots using a vacuum non consumable arc melting furnace, with the addition of C content increasing from 0 to 3.0 at. %. The weight of each ingot was 80 g, the diameter was 50 mm, and the height was 13 mm. Each ingot was remelted 4 times to ensure the uniformity of chemical composition. During each solidification process of melting, control the decrease in heating power at the same rate to eliminate the influence of solidification rate on the microstructure and mechanical properties. Each alloy ingot was detected for its actual composition, and the results were shown in Table 1.

Table 1. The actual composition of Ti45Al6NbxC alloysTi45Al6NbxC

Nominal composition	Actual composition			
	Ti (at. %)	Al (at. %)	Nb (at. %)	C (at. %)
Ti45Al6Nb	49.3	44.8	5.9	
Ti45Al6Nb1.0C	48.6	44.7	5.8	0.9
Ti45Al6Nb1.5C	48.3	44.7	5.7	1.3
Ti45Al6Nb2.0C	48.1	44.3	5.7	1.9
Ti45Al6Nb2.5C	47.5	44.5	5.7	2.3
Ti45Al6Nb3.0C	46.5	44.9	5.8	2.8

The six ingots were cut in the middle by electric discharge machining, and rectangular specimens were taken from half of the ingot, with a length of 20 mm, a width of 10 mm, and a height of 13 mm. The rectangular specimens were mechanical grinded and polished before being used for the preparation of metallographic specimens. The polished

metallographic specimens were placed in a corrosive solution (5% HF+15% HNO₃+80% H₂O vol.%) for 10 s to obtain qualified microstructures. The phase compositions of all alloys were tested and analyzed using a multifunctional X-ray diffractometer (XRD, model X'PERT). The copper target was used with a 2 θ measurement range of 0~167 $^{\circ}$, a controllable minimum step size of 0.0001 $^{\circ}$, and an angle measurement accuracy of $\pm 0.01^{\circ}$. The microstructures of the alloy were observed using field emission environmental scanning electron microscopy (SEM, model Quanta 200FEG) with energy dispersive spectroscopy (EDS) analysis function. The average size of lamellar colony was measured using the line cutting method. The microstructure of each sample was selected from 5 photos from different fields of view, and three data were measured on each photo. The final average lamellar colony size is the average of all data. The measurement of different constituent phases was carried out using the pixel measurement method in Photoshop software.

A cylindrical compressive specimen with a diameter of 6 mm and a height of 9 mm is cut from the other half of the ingot by electric discharge machining. The upper and lower cross-sections of the compressive specimen are polished to maintain their parallelism. The compression testing at room temperature was conducted on an electronic universal testing machine (model Instron 5569), with a set compression strain rate of 0.01 s⁻¹. On each component of the alloy ingot, three compressive specimens are cut, and the final compressive strength and compressive strain are the average values measured by the three tests.

3 Results and discussion

Fig. 1 shows the microstructures (SEM) of Ti₄₅Al₆Nb_xC alloys. According to Fig. 1(a), the microstructure of Ti₄₅Al₆Nb alloy includes large-sized lamellar colony, and a high content of white precipitate inside the lamellar colony. By observing Figs. 1(b)-1(f), it can be observed that after adding C element, the lamellar colony size is refined and short rod-shaped precipitate appears in the matrix. As the C content increases, the size of the lamellar colony decreases, and the content of white precipitate in the matrix also decreases. The content of short rod-shaped precipitate also increases with the increase of C content. By measuring the relative content of constituent phases and the size of lamellar colony, the effect of different C contents on the microstructure of Ti₄₅Al₆Nb alloy is further clearly declared. According to Table 2, as the C content increases from 0 to 3.5 at. %, the size of the lamellar colony decreases from 161.3 to 19.5 μm , the volume fraction of the white precipitate decreases from 10.4 to 1.4 vol. %, and the volume fraction of the short rod-shaped precipitate increases from 0 to 17.8 vol. %.

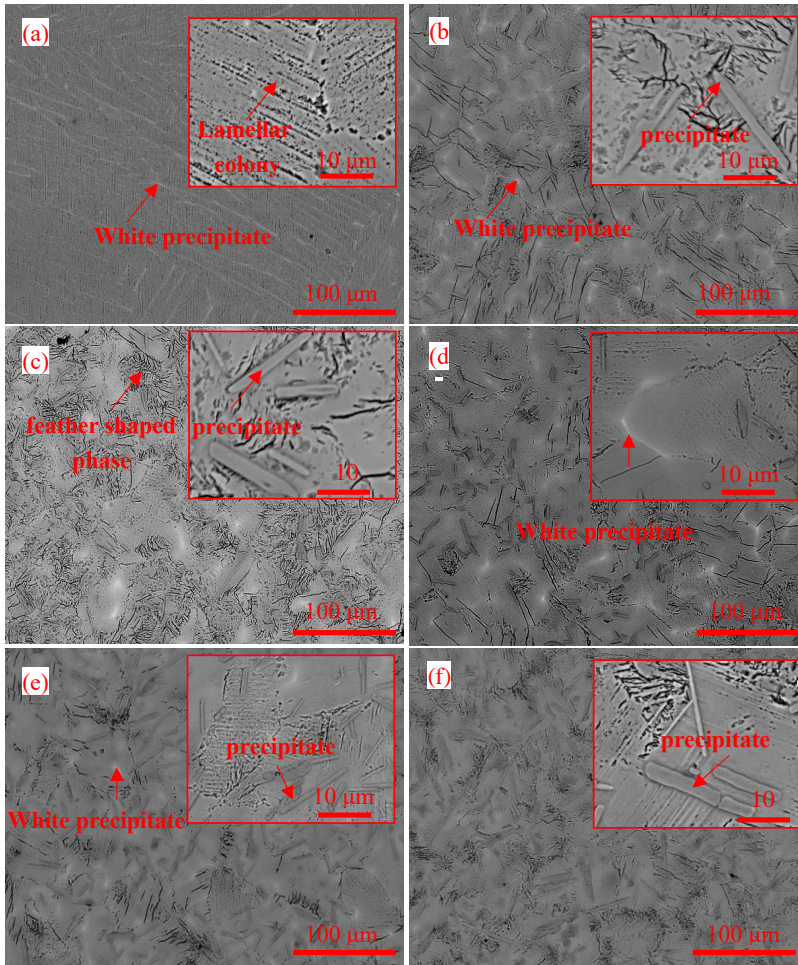


Fig. 1. Microstructures of Ti45Al6NbxC: (a) 0C; (b) 1.0C; (c) 1.5C; (d) 2.0C; (e) 2.5C; (f) 3.0C.

To further investigate the composition of phases in the TiAl matrix, especially the white precipitate and short rod-shaped precipitate, EDS is used to analyze various positions in the TiAl matrix. Fig. 2 shows the experimental results of EDS mapping scanning, line scan, and point analysis of various positions under the different C contents, and the composition of point analysis are shown in Table 3.

Table 2. The constituent phases and the average lamellar colony size of Ti45Al6NbxC alloys.

Alloy composition	Content of constituent phases/vol. %		Average lamellar colony/ μm
	white precipitate	short rod-shaped precipitate	
Ti45Al6Nb	10.4	0	161.3
Ti45Al6Nb1.0C	6.2	5.2	31.6
Ti45Al6Nb1.5C	5.1	6.8	25.2
Ti45Al6Nb2.0C	4.9	11.7	21.5
Ti45Al6Nb3.0C	3.6	15.1	19.8
Ti45Al6Nb3.5C	1.4	17.8	19.5

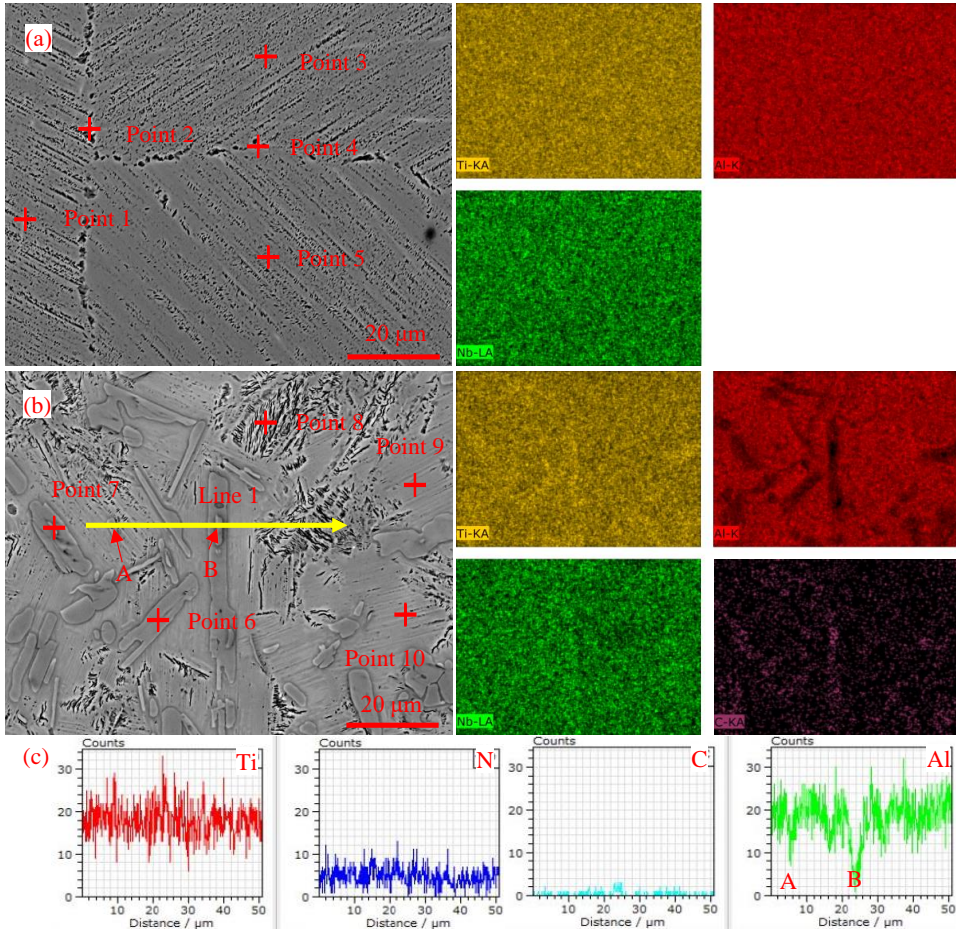


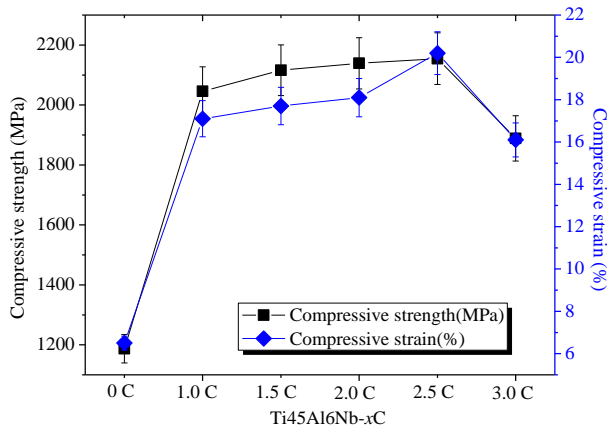
Fig. 2. EDS analysis of Ti45Al6NbxC alloys with different C content: (a) Mapping scanning and point analysis of Ti45Al6Nb alloy; (b) mapping scanning, line scanning, and point analysis of Ti45Al6Nb2.5C alloy; (c) experimental results of line scanning of Ti45Al6Nb2.5C alloy.

According to Fig. 2(b), numerous short rod-shaped precipitates appear in the Ti45Al6Nb3.0C alloy. The results of mapping scanning show that the short rod-shaped precipitates are enriched with C element instead of Al element. Through point analysis on Fig. 2(b), it is found from the results of points 8, 9, and 10 that the content of Nb in the matrix decreases, which is directly related to the addition of C element. Ti₂AlC phase is formed in the matrix due to the C addition and a portion of Nb solidly dissolves into Ti₂AlC phase, which reduces the Nb content in the matrix and the enrichment degree of Nb element in the matrix, ultimately leads to a decrease in the content of B2 phase. In the result at point 6, it is found that in the short rod-shaped precipitate, the atomic ratio of Ti, Al and C is close to 2:1:1. The chemical formula of the precipitate phase is Ti₂AlC, and a certain content of Nb is solidly dissolved in the Ti₂AlC phase. In the result at point 7, it is found that there are small-sized precipitates on the short rod-shaped Ti₂AlC phase, and the atomic ratio of Ti and C is close to 1:1, and the chemical formula of the precipitate phase is TiC, and a certain content of Nb is also solidly dissolved in the TiC phase. As shown in Fig. 2(c), when the line scanning passes through Ti₂AlC and TiC phases, there is a significant decrease in Al content, and this phenomenon becomes more obvious when passing through the TiC phase. The little change in Nb content also indicates that after adding C to form Ti₂AlC, the distribution of Nb element in the alloy matrix is relatively uniform.

Table 3. Composition of point analysis by EDS of Ti45Al6NbxC alloys.

Elements	Point 1	Point 2	Point 3	Point 4	Point 5	Point 6	Point 7	Point 8	Point 9	Point 10
Ti	53.6	53.3	56.8	49.9	54.1	52.7	49.8	50.5	51.9	54.5
Al	39.6	40.4	36.4	45.4	40.2	23.3	5.3	44.4	42.5	39.4
Nb	6.8	6.3	6.8	4.7	5.7	5.5	4.8	5.1	5.6	6.1
C	—	—	—	—	—	18.5	40.1	—	—	—

Fig. 3 shows the compressive properties at room temperature of Ti45Al6NbxC alloys. as the C content increases from 0 to 2.5 at. %, The compressive properties at room temperature of Ti45Al6NbxC alloy increases from 1186.9 to 2154.5 MPa, and the compressive strain increases from 6.5 to 20.2 %. As the C content further increases to 3.0 at. %, the compressive strength decreases from 2154.5 to 1888.7 MPa, and the compressive strain decreases from 20.2 to 16.1 %. According to previous literature reports [14], the Ti₂AlC/TiAl composite prepared by combustion synthesis reaction has a maximum compressive strength of 1835 MPa and a compressive strain of 16.4 %. With the increase of carbide content, the compressive properties no longer increase, and the compressive strength is less than 2000 MPa [15]. Therefore, the compressive properties at room temperature of the Ti45Al6Nb2.5C alloy obtained in this study are at a better level.

**Fig. 3.** The compressive properties at room temperature of Ti45Al6NbxC alloys.

Based on the above alloy microstructural analysis, several reasons for the improvement of mechanical properties of the alloy after adding C element can be summarized. Firstly, there is the precipitation strengthening effect. The addition of C element forms the short rod-shaped Ti₂AlC precipitate in the matrix, which withstands a certain load when the alloy is subject to the compression deformation process, thereby improving the alloy to withstand more loads. According to the shear lag model, when there are no reactants at the interface between the reinforcing precipitate and the matrix, the applied load on the matrix will be effectively transferred to the reinforcing precipitate, thereby improving the load bearing capacity of the alloy. As the C content increases, the content of Ti₂AlC precipitate in the round rod shape also increases, which can improve the mechanical properties at room temperature of the alloy to a certain extent. However, as a reinforcing phase, Ti₂AlC is difficult to deform, often resulting in numerous dislocations gathering around it. When dislocations aggregate to a certain extent, cracks will form and lead to cracking and ultimately fracture of the alloy. Therefore, the content of Ti₂AlC precipitate phase has an enhancing effect within a certain range, when it exceeds a certain content, the enhancing effect will weaken.

The grain-boundary strengthening is another significant factor. With the increase of C content, the size of the lamellar colony decreases, and the refined microstructure has more grain boundaries. The addition of C element generates in-situ Ti₂AlC particles in the liquid (approximately 1625 °C), and during the solidification process, Ti₂AlC particles act as

heterogeneous nuclei, increasing the number of heterogeneous nucleation sites at the solidification front and refining the size of lamellar colony [16]. When the accumulated dislocations reach a certain level, it will trigger the activation of dominant dislocation sources within adjacent grains, which will continue to cause dislocations and ultimately lead to alloy fracture. Therefore, an increase in the number of grain boundaries will more effectively hinder the movement of dislocations, thereby improving the mechanical properties of the alloy.

Finally, one of the main reasons affecting the mechanical properties of alloys is the content of B2 phase in the microstructure. B2 phase, as a hard phase, exists between the lamellar colony boundaries or within the lamellar colony. Under low temperature conditions, it often preferentially fractures, especially when the B2 phase are interconnected between the lamellar colony boundaries, which accelerates crack propagation. Therefore, reducing the content of B2 phase or eliminating B2 phase can effectively improve the mechanical properties of the alloy.

4 Conclusion

In this study, the effect of C on the content of B2 phase, lamellar colony size, the microstructure of Ti45Al6Nb alloy, the content of Ti2AlC reinforcing phase, the distribution of Nb element, and the compressive properties at room temperature are investigated. The effect mechanism of C element and its content on the microstructural evolution and mechanical properties has been revealed. In-situ Ti2AlC reinforcing phase is formed after adding C element. As the C content increases from 0 to 3.0 at. %, The content of Ti2AlC reinforcing phase increases from 0 to 17.8 vol. %, and the size of the lamellar colony decreases from 161.3 to 19.5 μm . Due to the heterogeneous nucleation of Ti2AlC formed in the liquid, the nucleation sites at the solidification front are increased, thereby refining the microstructure. B2 phase dissolved high content of Nb element is formed in the Ti45Al6Nb alloy. As the C content increases from 0 to 3.0 at. %, the content of B2 phase decreases from 10.4 to 1.4 vol. %. Ti2AlC reinforcing phase also dissolves a portion of Nb, promoting the uniform distribution of Nb elements in the TiAl matrix. As the C content increases from 0 to 2.5 at. %, the compressive strength at room temperature increases from 1186.9 to 2154.5 MPa, and the compressive strain increases from 6.5 to 20.2 %. Comprehensive factors for the improvement of compressive properties are precipitation strengthening of Ti2AlC, grain boundary strengthening of refined microstructure, and reduction of the content of B2 phase.

References

1. Y.L. Song, Z.H. Dou, T.A. Zhang, Y. Liu. *A novel continuous and controllable method for fabrication of as-cast TiAl alloy*, J. Alloy. Compd. **789**, 266-275 (2019).
2. L. Song, L. Wang, M. Oehring, X.G. Hu, F. Appel, U. Lorenz, F. Pyczak, T.B. Zhang. *Evidence for deformation twinning of the D0₁₉- α_2 phase in a high Nb containing TiAl alloy*, Intermetallics **109**, 91-96 (2019)
3. Y.L. Wu, R. Hu, J.R. Yang, Z.X. Jiao, P. Peng, *In-situ observation of microstructure evolution and phase transformation under continuous cooling in Ru-containing TiAl alloys*, Mater. Charact. **163** 110296 (2020)
4. G. Chen, Y. Peng, G. Zheng, Z. Qi, M. Wang, H. Yu, C. Dong, C.T. Liu. *Polysynthetic twinned TiAl single crystals for high-temperature applications*, Nat. Mater. **15(8)**, 876 (2016).
5. Y.H. Yu, H.C. Kou, Y.C. Wang, M.Y. Jia, X.X. Xu, Z.L. Zhao, Y.R. Wang, J.S. Li, *Formation of core-shell-like structure in β -solidified TiAl alloy and its effect on hot workability*, Acta Mater. **255** 119036 (2023).
6. W.J. Zhang, S.C. Deevi, G.L. Chen. *On the origin of superior high strength of Ti-45Al-10Nb alloys*, Intermetallics, **10(5)** 403-406 (2002).
7. H. Clemens, H. F. Chladil, W. Wallgram. *In-situ investigations of the β -phase in a Nb and Mo containing γ -TiAl based alloy*, Intermetallics **16(6)**, 827-833 (2008)
8. S.G. Tian, X.X. Lv, H.C. Yu, Q. Wang, Z.H. Jiao, H.F. Sun. *Creep behavior and deformation feature of TiAl-Nb alloy with various states at high temperature*, Mater. Sci. Eng. A **651** 490-498 (2015).
9. C.Z. Qiu, Y. L, W. Zhang, B. Liu, X.P. Liang. *Development of a Nb-free TiAl-based intermetallics with a low-temperature superplasticity*, Intermetallics **27(3)** , 46-51 (2012)

10. H. Clemens, H.F. Chladil, W. Wallgram, G.A. Zickler, R. Gerling, K.D. Liss, S. Kremmer, V. Güther, W. Smarsly. *In and ex situ investigations of the β -phase in a Nb and Mo containing γ -TiAl based alloy*, Intermetallics **16**(6) , 827-833 (2008)
11. D. Hu, A. Huang, X. Wu. *On the massive phase transformation regime in TiAl alloys: the alloying effect on massive/lamellar competition*, Intermetallics **15**, 327-332 (2007)
12. R. Benitez, H.L. Gao, M. O'Neal, P. Lovelace, G. Proust, M. Radovic. *Effects of microstructure on the mechanical properties of Ti₂AlC in compression*, Acta Mater. **143**, 130-140 (2018)
13. Z. Wu, R. Hu, T.B. Zhang, F. Zhang, H.C. Kou, J.S. Li. *Understanding the role of carbon atoms on microstructure and phase transformation of high Nb containing TiAl alloys*, Mater. Charact. **124**, 1-7 (2017)
14. S. Shu, F. Qiu, S. Lü, S. Jin, Q. Jiang. *Phase transitions and compression properties of Ti₂AlC/TiAl composites fabricated by combustion synthesis reaction*, Mater. Sci. Eng. A **539**, 344-348 (2012)
15. J. Lapin, A. Klimová, Z. Gabalcová, T. Pelachová, O. Bajana, M. Štamborská. *Microstructure and mechanical properties of cast in-situ TiAl matrix composites reinforced with (Ti,Nb)₂AlC particles*, Mater. Des. **133**, 404-415 (2017)
16. H.Z. Fang, R.R. Chen, Y. Yong, Y.Q. Su, H.S. Ding, J.J. Guo, H.Z. Fu. *Role of graphite on microstructural evolution and mechanical properties of ternary TiAl alloy prepared by arc melting method*, Mater. Des. **156**, 300-310 (2018)